

1 **Title:** More running causes more ocular dominance plasticity in mouse primary visual cortex:
2 new gated running wheel setup allows to quantify individual running behaviour of group-
3 housed mice.

4

5 **Abbreviated title:** More running, more ocular dominance plasticity

6

7 **Authors:** Cornelia Schöne^{1,2}, Jaya Sowkyadha Sathiyamani^{1,2,3}, Mihaela Guranda¹, Siegrid
8 Löwel^{1,2}

9

10 **Affiliation:**

11 [1] University of Göttingen, Department of Systems Neuroscience, 37075 Göttingen,
12 Germany
13 [2] Göttingen Campus Institute for Dynamics of Biological Networks, 37075 Göttingen,
14 Germany
15 [3] International Max Planck Research School for Neurosciences, 37075 Göttingen,
16 Germany

17

18 **Corresponding author:**

19 Cornelia Schöne

20 email: cornelia.schoene@gwdg.de

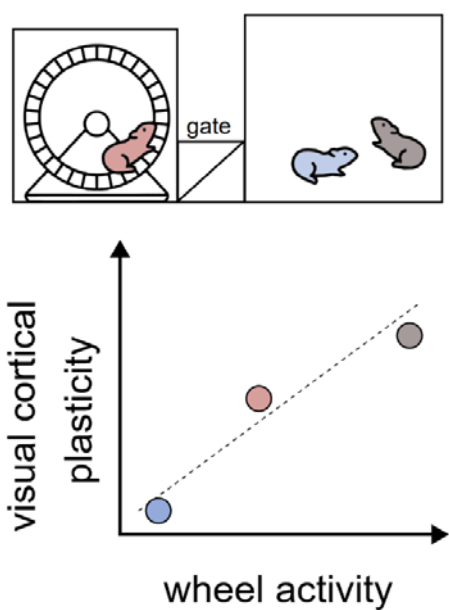
21 orcid: <https://orcid.org/0000-0003-2060-1084>

22

23

24 **Graphical abstract:**

25



With our newly developed gated running wheel setup, we observed a striking correlation between individual running activity, and a measure of experience dependent plasticity in mouse primary visual cortex. More running caused more plasticity: running speed, running distance, total running time, number of running bouts and bout duration all correlated with a measure of visual cortical plasticity, the ocular dominance index. Thus, our observations add to the growing body of evidence that individual behavioural choices strongly affect individual brain plasticity.

43

44

45 **Acknowledgements:** We thank DFG (SFB889, Project B05 to S.L.) and the Dorothea
46 Schröder-Program for funding. We thank Tobias Mühmer and Jan Hoffmann, for constructing
47 the gated running wheel cage, and Christina Ahlbrecht for technical assistance and animal
48 care.

49 **Title:** More running causes more ocular dominance plasticity in mouse primary visual cortex:
50 new gated running wheel setup enables individual tracking of wheel running in group-housed
51 mice.

52

53 **Abstract**

54 Environmental enrichment boosts neuronal plasticity of standard-cage raised (SC) mice.
55 Since it becomes increasingly more important to track individual mouse behaviours and its
56 influence on brain plasticity, we designed a gated running wheel (gRW) setup allowing to
57 correlate wheel running with neuronal plasticity, using the established paradigm of ocular
58 dominance (OD)-plasticity after monocular deprivation (MD).

59 After SC-rearing until adulthood (>P110), group-housed mice were transferred to gRW
60 cages, that provided an additional running wheel compartment for tracking individual wheel
61 activity via implanted RFID chips. Notably, individual running parameters varied enormously:
62 mice ran from close to 0 to ~20 km across the 7 days of gRW experience, with on average
63 running 0-3.96 km in 0-3.85 h/d and running bouts lasting from <1 up to 10 min, while
64 running at a speed of 6-26 cm/s. OD-plasticity in V1 after 7 days of MD in the gRW was
65 visualized using intrinsic signal optical imaging, and compared to control gRW-mice without
66 MD via calculation of an OD-index. Most, notably - while wheel running enabled OD-
67 plasticity - *individual* running parameters correlated with *individual* OD-indices after MD:
68 Mice running longer distances, for longer time, at higher speeds and with longer and more
69 frequent bouts displayed more experience-dependent V1-plasticity. In turn, a composite
70 measure of overall running wheel activity derived from principal component analysis of
71 running parameters accounted for 65% of inter-individual variability of OD-index following
72 MD. Together our study demonstrates that interindividual variability of running behaviour is
73 high, and mice intrinsically motivated to run more show enhanced V1-plasticity, underscoring
74 the huge importance of analysing individual behavioural parameters together with any
75 measure of brain plasticity. End

76

77 **Keywords:** Voluntary wheel running, ocular dominance plasticity, primary visual cortex,
78 inter-individual variability, behavioural tracking

79 Introduction

80 While the natural environment of humans and mice is complex, that of laboratory rodents
81 has been simplified and standardised in the past decades to an extent that deprives the
82 animals of essential behaviours (Löwel et al., 2017; Cait et al., 2024). For instance, standard
83 cage rearing (SC) leaves minimal room for the expression of individual traits and both
84 behavioural and physiological interindividual variability is further reduced by using inbred
85 strains lacking genetic variability (Wahlsten et al., 2006; Körholz et al., 2018). Recently, a
86 number of laboratories demonstrated that raising animals under less deprived rearing
87 conditions – in so-called “enriched environments”, i.e. housing in larger social groups and/or
88 larger cages, with regularly changed mazes to navigate through and running wheels for
89 voluntary physical exercise – elicits remarkable effects on brain wiring and plasticity across
90 molecular, anatomical, and functional levels when compared to animals raised in an SC
91 environment (Sale et al., 2007; Fabel et al., 2009; Baroncelli et al., 2010; Di Garbo et al.,
92 2011; Greifzu et al., 2014; Kalogeraki et al., 2014; Löwel et al., 2017; Stryker and Löwel,
93 2018; Bogado Lopes et al., 2023).

94 Both environmental enrichment, but also just voluntary wheel running have been shown to
95 boost experience-dependent changes in rodent primary visual cortex (V1) (Sale et al., 2007;
96 Baroncelli et al., 2010; Greifzu et al., 2014; Kalogeraki et al., 2014; Kaneko and Stryker,
97 2014), using the established model of ocular dominance (OD) plasticity after monocular
98 deprivation (MD) (Gordon and Stryker, 1996; Cang et al., 2005): when one eye is closed for
99 few days, the relative V1-activation strength is shifted towards the open eye (Cang et al.,
100 2005; Gordon and Stryker, 1996). SC-mice beyond P110 do no longer show OD-plasticity
101 with 7 days of MD (Lehmann and Löwel, 2008; Sato and Stryker, 2008), and need ~7 weeks
102 for V1-activation changes (Hosang et al., 2018)

103 While it is clearly established that running increases OD-plasticity in mice (Kalogeraki et al.,
104 2014; Kaneko and Stryker, 2014) the consequences of interindividual variability of wheel
105 running on experience-dependent V1-plasticity has not yet been studied. We therefore
106 aimed to analyse the effects of individual running behaviour on OD-plasticity of adult
107 (>P110) group housed SC-mice. As tracking individual wheel running activity of group
108 housed mice is still challenging (Mayr et al., 2020; Reuser et al., 2022), we designed a
109 custom-built gated running wheel (gRW) setup consisting of a rat-sized home cage
110 connected to a compartment with a surveyed running wheel that allowed individual tracking
111 of mice implanted with an RFID sensor. We quantified running distance, time, speed, bout
112 number and bout length of running activity and tested whether they correlated with the OD-
113 index, which compares visual stimulus evoked V1-activation via the ipsi- and contralateral
114 eye and thus quantifies the magnitude of OD-plasticity (Cang et al., 2005).

115 Running parameters varied extensively between individual mice, with some mice running
116 only few meters while others ran >20 km during their 7 days of running wheel exposure.
117 Most notably, correlating the macro (running distance, time and speed) and micro (bout
118 number and duration) architecture of running wheel activity of individual mice with their
119 individual OD-index, quantifying OD-plasticity, revealed strong correlations with Pearson
120 correlation coefficients ranging from -0.77 to -0.83: more active runners displayed stronger
121 OD-plasticity. Our results underscore the importance of taking individual behavioural choices
122 into account when analysing influences on brain plasticity.

123 Methods:

124 Animals and rearing conditions

125 In order to avoid conflict between group housed males, we limited our experiments to groups
126 of 2-5 adult female C57Bl6/J mice (age range P127-225, called P160), growing up in
127 Tecniplast 1284 standard mouse cages (SC; size: 17x32x19cm) until the day an MD/noMD
128 was performed. After the MD/noMD, animals were cohoused in the gRW-setup, provided
129 with *ad libitum* food and water, and maintained on a 12 h light dark cycle.. All experimental
130 procedures complied with the National Institutes of Health guidelines for the use of
131 laboratory animals and were approved by the local government of Lower Saxony, Germany
132 (Niedersächsisches Landesamt für Verbraucherschutz und Lebensmittelsicherheit).

133 Optomotry, monocular deprivation and implantation of RFID 134 tags

135 To ensure that all experimental mice had regular vision before testing OD-plasticity with MD,
136 we measured the spatial frequency threshold (SFT) of the optomotor reflex of both eyes
137 using an optomotor system (Prusky et al. 2004; Lehmann and Löwel, 2008). SFT values
138 were within published values and differed by less than 0.02 cyc/deg between the two eyes in
139 all mice.

140 Thereafter, the right eye was sutured shut (MD) for 7 d according to published protocols
141 (Gordon and Stryker, 1996; Cang et al, 2005; Greifzu et al., 2014). In brief, mice were
142 anaesthetized using 2.5 % isoflurane in 1:1 O₂/N₂, and kept at 1-1.5% isoflurane for stable
143 anaesthesia. Body temperature was maintained at 37°C using a heat pad and rectal probe.
144 After subcutaneous injection of Rimadyl (Carprofen, 5 mg/kg) and covering of eyes with
145 Bepanthen eye cream, a local analgesic (Lidocaine, xylocaine gel 2 %, Aspen Pharma
146 Trading Limited, Ireland) was applied to the eyelid of the right eye before trimming and
147 closing of the eye with 2 mattress stiches (suture material: 7-0 Perma-Hand silk, Ethicon,
148 8.0mm diameter). The eyes of the animals were examined daily to ensure that the MD-eye
149 stayed closed. Additionally, optomotor reflex thresholds (SFT) of the open eye were tested
150 daily after MD, as a measure for functional MD, including the day of intrinsic signal optical
151 imaging.

152 Cylindrical glass-covered radio frequency identification devices (RFID; length: 12.5 mm;
153 diameter: 1.93 mm, Sparkfun Electronics, Colorado, USA) were implanted during the MD or
154 noMD (control without MD) surgery to minimize mouse discomfort. First, a patch of fur was
155 shaved in the animal's neck using small surgical scissors, then a local analgesic gel
156 (Lidocaine, xylocaine gel 2 %, Aspen Pharma Trading Limited, Ireland) was applied to the
157 exposed skin. A small incision was made and the chip carefully placed subcutaneously in the
158 scruff to make it difficult for the mice to pick at and thereby reducing the risk of an infection.
159 The incision was sealed with a simple interrupted stitch (suture material: 7-0 Perma-Hand
160 silk, Ethicon, 8.0mm diameter). After MD/RFID implantation and complete recovery from
161 anaesthesia, mice were moved to a gRW setup.

162 Gated running wheel setup (gRW)

163 In order to assess individual running wheel behaviour, we developed an open source gated
164 running wheel (gRW) cage, which served as the home cage for the duration of the
165 experiment (Figure 1A, Table 1). It consisted of a standard size rat cage (43cm x 27cm)
166 connected to a separate gRW-compartment, equipped with the same RW as used in the
167 enrichment cages in Greifzu et al., 2014 (Figure 1A). Wheel diameter was 12.5 cm, so that
168 the calculated RW-circumference was 39.3 cm. RW-turns were registered using a hall
169 sensor for detecting motion of two magnets attached at opposing sites of the RW. The mice
170 needed to pass through a seesaw in order to reach the RW-compartment. Entering would
171 flip the seesaw blocking other mice from entering (see video 1 and 2). To ensure the seesaw
172 remained closed while a mouse was inside the RW-compartment, the seesaw was actively
173 blocked from flipping back. When activity was detected by beam break sensors outside the
174 RW-compartment, an electromagnet was activated to hold the seesaw closed. Attempts of
175 mice to exit the RW-compartment were detected using beam break sensors inside the RW-
176 compartment, which would deactivate the seesaw magnet. Seesaw position was registered
177 through a roller switch.

178 Mice were chipped with radio frequency identification devices (RFID). The RFID-tags
179 transmitted the encrypted individual ID to a USB-driven reading device (ID-20LA SparkFun
180 Electronics, Colorado, USA) at 125 kHz via a custom-made RFID coil. Thus, each time a
181 mouse passed underneath the RFID coil into the gRW compartment, RFID and time stamps
182 were saved. All sensors were connected to the GPIO pins of a raspberry pi 4B+. In addition,
183 a raspberry pi noir camera was used to record movement inside the RW-compartment at 40
184 Hz; camera data were used to confirm sensor data and to extract RW-turns when the Hall
185 sensor failed. All data was recorded using custom written python scripts running on the
186 raspberry pi. A 3D .pdf file illustrating dimensions of cage components and electronic
187 assembly is provided under supplementary material (Model 1 and Figure S1, respectively).

188 Analysis of gated wheel running

189 In order to assign each RW-turn to individual mice, we first defined running bouts as running
190 at a speed above 0.1 Hz, then the most recently detected RFID was assigned to all wheel
191 turns within the respective running bout. When more than one RFID was detected since the
192 last gate flip, this indicated that more than one mouse had entered the gRW compartment.
193 This occasionally happened, due to two mice squeezing through the gate simultaneously, or
194 due to failure of the magnetic seesaw lock. In this case, the RW-turns were labelled as
195 ambiguous. Mice with ambiguous RW-turns of more than 7% were excluded from the RW-
196 analysis, but included for analysis of OD-plasticity in Figure 2. For the remaining mice, on
197 average, we quantified $1.7 \pm 0.5\%$ ambiguous RW-turns (n=20 mice), confirming that the self-
198 locking seesaw of the gRW was well suited to restrict access to the wheel compartment to
199 individual mice.

200 Optical imaging of intrinsic signals and visual stimuli.

201 As a final step of the experiment, OD-plasticity was assessed after 7 days of MD/noMD in
202 the gRW-setup, using optical imaging of intrinsic signals (Cang et al., 2005; Greifzu et al.,
203 2014).

204 *Surgery.* Briefly, mice were box-anaesthetised with 2.5% halothane in O₂ and N₂O (1:1) and
205 injected with atropine (5mg/kg, s.c.; Franz Köhler Chemie), dexamethasone (8mg/kg s.c.;
206 Merck), and chlorprothixene (8mg/kg, i.m.; Sigma-Aldrich). After placing animals in a
207 stereotaxic frame, anaesthesia was maintained with 0.8% halothane in a 1:1 mixture of O₂
208 and N₂O.

209 *Data acquisition and visual stimulation* (Kalatsky and Stryker, 2003; Cang et al, 2005).
210 Mouse V1 responses were recorded through the skull using the “Fourier” imaging method of
211 Kalatsky and Stryker (2003) and optimised for the assessment of OD-plasticity (Cang et al.,
212 2005). V1-signals were visualised with a CCD camera (Dalsa 1M30) using a 135x50 mm
213 tandem lens configuration (Nikon) with red illumination light (610±10 nm). Active brain
214 regions absorb more red light and appear darker in the images. Frames were acquired at a
215 rate of 30 Hz, temporally binned to 7.5 Hz, and stored as 512x512-pixel images after spatial
216 binning of the camera image. Visual stimuli were presented on a 60 Hz refresh rate monitor
217 (21 inches; Accuvue HM-4921-D, Hitachi) positioned 25 cm from the eyes. Stimuli consisted
218 of white drifting horizontal bars (2° wide) limited to the contralateral binocular visual field (-5°
219 to 15°) as described previously (Greifzu et al., 2014). The amplitude component of the
220 optical signal represents the intensity of neuronal activation (expressed as fractional change
221 in reflectance times 10⁻⁴) and was used to calculate an ocular dominance (OD) index. At
222 least three maps per animal were averaged by an experimenter blinded to the experimental
223 conditions to compute the OD-index as (C+I)/(C-I), with C and I representing the response
224 magnitudes of each pixel to visual stimulation of the contralateral (C) and ipsilateral (I) eye.

225 EXPERIMENTAL DESIGN AND STATISTICAL ANALYSES

226 Principal component analysis

227 Principal component analysis was performed using the MATLAB (R2022b) pca function on
228 wheel running parameters (distance, time, speed, bout duration and bout number) obtained
229 from combined noMD and MD mice in order to eliminate multicollinear variables which
230 effectively reduces dimensions of descriptive variables with the first principal component
231 (PC1) capturing the maximum variance of the data (86-90% of variance in wheel running
232 parameters, depending on whether average or individual data across days was used,
233 respectively). In both cases, PC1 had the biggest loading for bout no., with smaller loadings
234 for all other wheel parameters (Figure S2). Together this suggests, that PC1 is well suited to
235 represent overall wheel activity capturing maximal variance of individual running wheel
236 performance.

237 Statistical analysis

238 Normality of data was assessed using the Kolmogorov-Smirnov test, and non-parametric
239 versus parametric tests were chosen accordingly as stated in the text. Inter-group
240 comparisons between two groups were done by Student's t-test or Mann Whitney test, for 3
241 or more groups, we used one or two-way analysis of variance (ANOVA), as detailed. In
242 analyses in which a within-subject factor was present (i.e. eye), ANOVA with repeated
243 measurements was performed. Post hoc multiple comparison tests were corrected by
244 applying Sidak correction to p-values. The levels of significance were set as *: p<0.05; **:
245 p<0.01; ***: p<0.001. Data are represented as means ± standard error of mean (s.e.m.).

246 **Software accessibility**

247 Any software and code used for running the gRW setup and for processing obtained data
248 are available upon request.

249 **Results**

250 **The gated running wheel setup allows for detailed readout of
251 individual mouse running behaviour.**

252 Given the importance of social interactions for the well-being of mice, we specifically
253 designed a gated running wheel setup (gRW), so that we could track individual running
254 activity of group-housed mice in a home cage setting. The gRW setup consists of a standard
255 rat cage connected to a separate compartment with a running wheel for voluntary physical
256 exercise (Figure 1A). Upon entering the gRW-compartment, mice are individually registered
257 using an implanted RFID sensor allowing to allocate running bouts to individual animals. This
258 enables us to quantify individual wheel running parameters and to correlate individual
259 running behaviours with individual V1-plasticity parameters assessed using intrinsic signal
260 optical imaging.

261 In order to provide a detailed analysis of wheel activity of mice, we first compared running
262 wheel activity between animals undergoing monocular deprivation (MD, n=12) and control
263 mice (noMD, n=8): wheel running was not affected by MD (Figure S2). Next, we evaluated
264 whether the separate gRW-compartment would impair access and reduce overall running
265 activity compared to a previous publication using identical running wheels located inside the
266 home cage. This did not seem to be the case: mice in the gRW setup ran 3307 ± 763 RW
267 turns per day, corresponding to 1.3 ± 0.3 km/d (Figure 1B), rather similar to the 3991 ± 445 RW
268 turns/day, corresponding to 1.6 ± 0.2 km/d of the animals of a previous study (Kalogeraki et
269 al., 2014).

270 Since, typically, only a single mouse entered the RW compartment at a time, the activity of
271 individual mice could be well separated by assigning running bouts to individual mice for
272 assessing interindividual variability in wheel running (Figure 1C-G). Across mice, running
273 distance increased over days as revealed by linear regression analysis (Figure 1D,
274 $F(1,138)=4.98$, $p=0.027$). However, running was not consistent across days for individual
275 mice (Figure 1D), and could range from close to 0 to above 10 km on individual days and for
276 individual mice (Figure 1D). Average cumulative running distances reached 8.2 ± 1.8 km after
277 7 days, ranging from close to 0 to above 20 km of total distance travelled by individuals
278 (Figure 1D). Mice exhibited a significant increase in running distance from day 1 to day 7
279 (Figure 1E, one-sample t-test $p=0.001$), whereas the difference between day 4 and day 1
280 was not significant (Figure 1E). This was paralleled by a larger proportion of mice running
281 more than one bout per day, which increased from 50% on day 1 to 75% on day 7 (Figure
282 1F).

283 As expected from nocturnal animals, mice ran more during night time compared to day time,
284 with approximately 50% of mice showing a clear circadian pattern and running predominantly
285 during night time (Figure 1F), while the other half of the animals did not run sufficiently to
286 detect circadian activity preferences, and few individuals also occasionally ran during day
287 time.

288 On average, mice achieved running times of 1.5 ± 0.3 h/d consisting of 17 ± 3 bouts/d with
289 individual running bouts lasting on average 5.0 ± 0.5 min, while running at a speed of 18 ± 1
290 cm/s (Figure 1G). Of note, mice covered a wide range of running wheel parameters, running
291 $0.3\text{--}3.96$ km/d in $0.3\text{--}3.85$ hours with running bouts lasting from <1 up to 10 min, while running at
292 a speed of $6\text{--}26$ cm/s. Interestingly, mice running longer distances typically also spent more
293 time running, at faster speeds, which was also reflected in a larger number of running bouts,
294 with few exceptions, as illustrated by the colour coding of individuals in figures 1E,G. A
295 correlation matrix was computed to examine the interrelationships between the 5 quantified
296 running parameters more precisely (Figure H): The strongest correlation was observed
297 between distance and time ($R=0.97$, $p<0.0001$), i.e. mice that ran for longer time periods also
298 travelled a larger total distance. Speed and bout number also strongly correlated with running
299 distance (speed: $R=0.81$, $p<0.0001$; bout no: $R=0.72$, $p<0.0001$), i.e. mice running faster and
300 more often, also reached a higher final distance. In turn, bout duration did not correlate with
301 distance, time or number of bouts ($p>0.05$), however there was a significant correlation with
302 running speed ($R=0.63$, $p<0.01$), i.e. faster mice also ran longer bouts.

303 Together, these data demonstrate i) substantial interindividual variability in multiple running
304 wheel parameters of our group-housed mice which may influence cortical plasticity, and ii)
305 that our new gRW-setup is ideally suited to analyse this question in detail.

306 Gated wheel running restores OD-plasticity to adult standard 307 cage raised mice

308 We had previously shown that running can boost OD-plasticity in SC-raised adult mice, even
309 if running was possible only during 7 days of MD (Kalogeraki et al., 2014). Here, we tested
310 whether i) the gRW setup also boosts OD-plasticity in SC-mice and ii) individual running
311 parameters, i.e. running more, would influence individual OD-plasticity. gRW-housing started
312 immediately after MD, and V1-activity maps were visualized after 7 days of MD. We
313 recorded intrinsic signal optical imaging responses of binocular V1 to visual stimulation of
314 the left and right eye with horizontal drifting bars (Cang et al., 2005).

315 Confirming previous imaging data in mice without MD (Lehmann and Löwel, 2008; Sato and
316 Stryker, 2008), visual stimulation of the contralateral eye induces a stronger V1-activation
317 compared to ipsilateral eye stimulation, visible as darker patches in the V1-activity maps
318 (Figure 2A), and reflected in a higher V1-activation strength (Figure 2C; contra/ipsi:
319 $2.0 \pm 0.2/1.3 \pm 0.1$, $n=10$, $p=0.0003$). In contrast, in gRW mice, MD induced a clear OD-shift:
320 After MD, the contralateral eye no longer activated V1 more strongly than the ipsilateral eye
321 (contra/ipsi: $1.7 \pm 0.2/1.5 \pm 0.2$, $n=9$; $p=0.7$). Calculating the OD-index, quantifying OD-
322 plasticity by comparing ipsi- and contralateral eye induced V1-activity (Fig. 2B), confirms the
323 gRW boosted OD-shift: in noMD mice, the OD-index was 0.24 ± 0.04 ($n=10$), indicating
324 contralateral eye dominance, whereas following MD, the OD-index was reduced to
325 0.05 ± 0.04 ($n=9$, Mann-Whitney p -value 0.001), demonstrating a clear OD-shift in P160 mice.
326 Thus, our new gRW setup boosts OD-plasticity in group-housed mice.

327 328 Optomotor results

329
330 To test animals' basic visual abilities and to confirm the effectiveness of MD, we used the
331 virtual reality optomotor system, and measured the spatial frequency threshold (SFT) of the
332 optomotor reflex before and after MD (Prusky et al., 2004): vertical drifting gratings of

333 various spatial frequencies evoke small horizontal head and neck movements following the
334 stimulus. MD typically leads to an enhancement of optomotor reflex thresholds through the
335 open eye (citation!). Confirming effective MD, the SFT of our group-housed mice increased
336 from 0.39 ± 0.00 cyc/deg on day 0 to 0.51 ± 0.00 cyc/deg on day 7 after MD ($n=10/9$; 2-way
337 ANOVA for effect of MD $p < 0.0001$; Figure 2H), while values remained stable in noMD mice
338 (day 0/7: $0.39 \pm 0.00/0.39 \pm 0.00$ cyc/deg, 2-way ANOVA for effect of MD: $p < 0.0001$).

339 **Gated running wheel parameters correlate with a measure of
340 ocular dominance (OD) plasticity, the OD-index**

341 *Correlation of overall running wheel activity with OD-index:* In order to investigate how
342 individual behavioural choices shape brain plasticity, we tested whether individual running
343 wheel parameters were correlated with individual OD-indices, which quantify the magnitude
344 of OD-plasticity. For this, we first obtained a measure of overall gRW activity for individual
345 mice by performing a principal component analysis (PCA) on the quantified running wheel
346 parameters (distance, time, speed, running bout numbers, bout duration) of pooled no MD
347 and MD mice, averaged across the 7 days of wheel exposure. The first principal component
348 explained 87% of interindividual variability in wheel running and hence was a suitable
349 measure of overall gRW activity of individual mice (see methods and figure S2 for details).
350 Strikingly, interindividual variability in gRW activity explained 65% of variability of the OD-
351 index ($r^2=0.65$, $p=0.017$, Figure 3A,B): Animals with high gRW performance showed a lower
352 OD-index and thus increased plasticity (Figure 3A,B). In contrast, correlation analyses in no
353 MD mice revealed no significant relationship between gRW activity and OD-index ($r^2=0.02$,
354 $p=0.77$, Figure 3B).

355 *Correlation of individual running wheel parameters with OD-index:* In addition, we also
356 observed striking correlations of individual running wheel parameters with individual OD-
357 index after MD (Figure 3C). In MD mice, bout duration, speed, bout number, running
358 distance and running time explained close to or above 60% (e.g. $r^2 \geq 0.60$) of the
359 interindividual variability in OD-index of MD mice ($n=9$; bout duration: $r^2=0.69$, $p=0.0102$;
360 speed: $r^2=0.63$, $p=0.0175$; bout no: $r^2=0.58$, $p=0.0271$; running distance: $r^2=0.60$, $p=0.0243$;
361 running time $r^2=0.62$, $p=0.0192$). Importantly, no significant correlation between running
362 wheel parameters and OD-index was found in the no MD control group ($p > 0.05$ for all
363 parameters), suggesting that baseline OD-index is not affected by wheel running.

364 *Correlation of wheel activity on specific days with OD-index:* Previous experimental evidence
365 has demonstrated that running wheel activity correlates with cortical gamma activity in V1
366 (Niell & Stryker, 2010), and that MD is associated with increased gamma activity in V1 for
367 several hours after MD, at least in juvenile mice aged 24-27 days (Quast et al., 2023).
368 Hence, we wondered whether running wheel activity on a specific day after MD was
369 correlated more strongly with the OD-index. For this we used PCA for dimensionality
370 reduction of running wheel parameters measured for *each day separately* and correlated the
371 first principal component (explaining 90% of variability of running wheel parameters across
372 days and animals) with the OD-index: gRW activity significantly correlated with the OD-index
373 on days 6 and 7 after MD (day6/7: $r^2=0.52/0.53$, $p=0.045/0.041$), while this relationship was
374 not significant on days 1-5 ($p > 0.05$ for all correlations), suggesting that predominantly
375 running on days 6 and 7 affects the OD-index. Nevertheless, gRW activity on the first days
376 still contributed to individual variability in OD-index, since including gRW activity of
377 cumulative numbers of days in the analysis already produced significant correlations when

378 only data from days 1 and 2 was included ($p>0.05$ for day 1 alone, $p<0.05$ for data from >1 days).

380 Overall these data document that group housed mice display huge interindividual variability
381 in voluntary physical exercise when given the possibility to use a running wheel: individuals
382 differ in bout number, bout duration, running speed, running distance and running time. Most
383 notably, the amount of wheel running was predictive of the magnitude of OD-plasticity: Mice
384 that ran more had stronger experience-dependent changes in V1-activation after MD. This
385 directly highlights the importance of inter-individual behavioural variability for brain plasticity
386 and suggests that individual behavioural choices and their influence on brain physiology and
387 plasticity should be an integral part of future studies.

388 Discussion

389 Using our newly developed gated running wheel setup (gRW) that allows to track individual
390 running parameters of group-housed mice, we observed an enormous variability of individual
391 behaviours of the tested animals: running speed, running distance, total running time,
392 number of running bouts and bout duration varied by many orders of magnitude between
393 individuals. Furthermore, we revealed a striking correlation between individual running
394 parameters and experience-dependent plasticity in mouse V1. More running caused more
395 ocular dominance (OD) plasticity: all quantified running parameters significantly correlated
396 with a measure of visual cortical plasticity, the OD-index. Thus, our observations add to the
397 growing body of evidence that individual behavioural choices can strongly affect individual
398 brain plasticity, and should therefore be considered when analysing neuronal plasticity.

399
400 Mice housed in the gRW for one week showed huge interindividual differences in running
401 wheel performance, running 0-3.96 km/d in 0-3.85 hours with running bouts lasting between
402 0 and 10 min, while running at a speed of 6-26 cm/s, suggesting diverse intrinsic motivation
403 to run. Wheel running is distinct from home cage running because the distances and speeds
404 reached per day are drastically increased when mice have access to a running wheel. Mice
405 in their home cages only achieve speeds of up to 1 cm/s and distances of 0.1-0.2 km/d
406 (Iannello, 2019), while for running wheels allow speeds of up to 15-120 cm/s and distances
407 of 1-20 km/d have been reported (Koteja et al., 1999; Kopp, 2001; Manzanares et al., 2018).
408 While our data spans the lower end of the reported range - with individual mice running up to
409 10 km/d on single days – this is expected from the specific conditions used here: i) group
410 housing reduces running distances by ~50% (Plenz and Kanold, 2021) and ii) the short-term
411 wheel access provided here for only 7 days likely was not sufficient for mice to reach a
412 stable performance, which has been reported to take ~2 weeks (De Bono et al., 2006).

413
414 It is widely accepted that OD-plasticity in SC-raised mice is age-dependent, with clearly
415 decreasing plasticity in adult animals beyond P110, which requires an extended MD for
416 observable OD-shifts (Sawtell et al., 2003; Pham, 2004; Hofer et al., 2006; Lehmann and
417 Löwel, 2008; Sato and Stryker, 2008; Hosang et al., 2018). A number of environmental and
418 behavioural interventions have been established by now for restoring plasticity in adult SC-
419 raised rodents or for sustaining the plastic potential of adult rodent V1 beyond that age
420 (Espinosa and Stryker, 2012; Hübener and Bonhoeffer, 2014). This includes previous
421 episodes of MD (Hofer et al., 2006), forced visual stimulation (Matthies et al., 2013),
422 combined visual stimulation and running (Kaneko and Stryker, 2014), and dark rearing (He

423 et al., 2006; Stodieck et al., 2014), all of which promoted visual cortical plasticity in adult
424 animals. Notably, mice and rats with access to a running wheel or housing in enriched
425 environment retained OD-plasticity into late adulthood (Sale et al., 2007; Baroncelli et al.,
426 2010; Greifzu et al., 2014; Kalogeraki et al., 2014), demonstrating that voluntary physical
427 exercise can sustain the brain's capacity for adaptive modification to environmental changes.
428

429 While OD-shifts obtained in the present gRW-mice were similar to previously published data
430 after 7 days of RW-enrichment (Kalogeraki et al., 2014), OD-shifts were smaller compared to
431 animals experiencing lifelong enrichment in even larger 2-floor cages with a regularly
432 changed maze (Greifzu et al., 2014). Thus, while short-term running can restore OD-
433 plasticity in adult mice, more complex enrichment of their immediate environment for longer
434 periods of time, enables stronger experience-dependent V1-activity changes. Alternatively,
435 extension of MD-duration can also boost OD-plasticity in adult SC mice (Hosang et al.,
436 2018). Thus, there seems to be a trade-off between age and MD duration in SC-raised
437 animals: in younger mice, shorter MDs are sufficient to induce significant OD shifts. In
438 contrast, older SC-mice need considerably extended MD duration to display OD plasticity,
439 but these long MD times can be shortened by specific environmental and behavioural
440 interventions such as, e.g., raising animals in an enriched environment (Sale et al., 2007;
441 Greifzu et al., 2014) or providing access to a running wheel (Kalogeraki et al., 2014), like in
442 the present study.

443
444 Using C57Bl/6J inbred mice housed in the gRW-setup allowed us to test how individual
445 behavioural trajectories affect brain plasticity with minimal influence of genetics on the
446 observed phenotype. In line with the model of Kempermann (2019), we observed a linear
447 relationship between running parameters and OD-plasticity quantified by the OD-index, with
448 individual running performance predicting up to 65% of phenotypic variability in OD-index
449 between mice. Thus, individual behavioural choices exert a strong influence on experience-
450 dependent plasticity. Interestingly, all wheel parameters correlated similarly strong with
451 individual OD-index, with p-values of correlations only varying slightly between 0.010 and
452 0.027 between bout duration, bout number, running speed, running distance and running
453 time. As wheel running comprises a rewarding behaviour that even mice in the wild pursue
454 voluntarily (Sherwin, 1998), it remains unclear why some mice showed very little wheel
455 activity. Multiple factors affecting wheel running have been identified, including mouse strain,
456 sex, group housing, social hierarchy, age and circadian rhythms (Kopp, 2001; De Bono et
457 al., 2006; Basterfield et al., 2009; Bartling et al., 2017; Bains et al., 2018; Balog et al., 2019;
458 Plenz and Kanold, 2021). Importantly, social hierarchy has been shown to affect both wheel
459 running and OD-plasticity in male mice, with dominant males exhibiting stronger OD-shifts
460 compared to subordinate males (Balog et al., 2019). While social hierarchies are less
461 prominent in female mice (Williamson et al., 2019) used here, we cannot exclude that
462 subordinate social rank may have caused reduced access to the gRW in some of our mice,
463 and thus might have contributed to both the amount of wheel running and variability of OD-
464 index.

465
466 Both high running speed and bout duration require high physical fitness and might be
467 associated with better sensory-motor coordination for efficient running that may improve with
468 practice (De Bono et al., 2006), suggesting that pre-training or rearing under less deprived
469 conditions could also benefit OD-plasticity by enabling more efficient running and higher
470 fitness. Interestingly, as intermittent access to running wheels has been shown to specifically

471 increase adult neurogenesis in the hippocampus as opposed to continuous long term access
472 (Nguemeni et al., 2018), gRW housing might provide additional benefits as wheel access
473 was limited to one mouse at a time.

474
475 In addition, variability in the activity of specific neural networks has been linked to mouse
476 wheel activity (Rhodes et al., 2003): lateral hypothalamic orexin/hypocretin and GAD65
477 networks have emerged as drivers of locomotion initiation (Kosse et al., 2017; Karnani et al.,
478 2020), suggesting that interindividual differences in network activity might explain variability
479 in wheel running. In addition, other factors which were not captured in our experiment, might
480 also have contributed to variability in OD-plasticity. This includes exploratory behaviours not
481 captured by our setup, a higher intrinsic plastic ability of the brain enabling OD-plasticity
482 more independently of external factors, which might be related to overall higher fitness levels
483 as also suggested by younger mice running more than older mice (Bartling et al., 2017).

484
485 Together, our newly developed gRW-setup allowing to correlate individual mouse running
486 behaviour with individual measures of experience-dependent V1-plasticity has demonstrated
487 a striking correlation between mouse running activity and OD-plasticity, highlighting the
488 importance of individual behavioural tracking for explaining experimental data. Thus, our
489 observations add to the growing body of evidence that individual behavioural choices can
490 strongly affect individual brain plasticity and thus should be analysed more carefully in future
491 studies.

492
493 **Author contributions:** Study design by C.S. Data collection and initial processing by C.S.,
494 J.S and M.G. Formal analysis by C.S. Data interpretation by C.S. and S.L. Original
495 manuscript draft by C.S. Reviewing and editing of manuscript draft C.S. and S.L.

496
497 **Conflict of Interest Statement:**
498 The authors whose names are listed above certify that they have NO affiliations with or
499 involvement in any organization or entity with any financial interest (such as honoraria;
500 educational grants; participation in speakers' bureaus; membership, employment,
501 consultancies, stock ownership, or other equity interest; and expert testimony or patent-
502 licensing arrangements), or non-financial interest (such as personal or professional
503 relationships, affiliations, knowledge or beliefs) in the subject matter or materials discussed
504 in this manuscript.

505
506 **Data Availability Statement:**
507 The data supporting the findings of this research are available on request to the
508 corresponding author, pending a formal data-sharing agreement and approval from the local
509 ethics committee.

510
511 **Acknowledgements:** We thank DFG (SFB889, Project B05 to S.L.) and the Dorothea
512 Schröder-Program for funding. We thank Tobias Mühmer and Jan Hoffmann, for constructing
513 the gated running wheel cage, and Christina Ahlbrecht for technical assistance and animal
514 care.

515 References

- 516
517 Bains RS, Wells S, Sillito RR, Armstrong JD, Cater HL, Banks G, Nolan PM (2018)
518 Assessing mouse behaviour throughout the light/dark cycle using automated in-cage
519 analysis tools. *J Neurosci Methods* 300:37–47.
- 520 Balog J, Hintz F, Isstas M, Teichert M, Winter C, Lehmann K (2019) Social hierarchy
521 regulates ocular dominance plasticity in adult male mice. *Brain Struct Funct*
522 224:3183–3199.
- 523 Baroncelli L, Sale A, Viegi A, Maya Vetencourt JF, De Pasquale R, Baldini S, Maffei L (2010)
524 Experience-dependent reactivation of ocular dominance plasticity in the adult visual
525 cortex. *Exp Neurol* 226:100–109.
- 526 Bartling B, Al-Robaiy S, Lehnich H, Binder L, Hiebl B, Simm A (2017) Sex-related
527 differences in the wheel-running activity of mice decline with increasing age. *Exp*
528 *Gerontol* 87:139–147.
- 529 Basterfield L, Lumley LK, Mathers JC (2009) Wheel running in female C57BL/6J mice:
530 impact of oestrus and dietary fat and effects on sleep and body mass. *Int J Obes*
531 33:212–218.
- 532 Bogado Lopes J, Senko AN, Bahnsen K, Geisler D, Kim E, Bernanos M, Cash D, Ehrlich S,
533 Vernon AC, Kempermann G (2023) Individual behavioral trajectories shape whole-
534 brain connectivity in mice Lerch JP, Behrens TE, Lerch JP, Yee Y, eds. *eLife*
535 12:e80379.
- 536 Cait J, Winder CB, Mason GJ (2024) How much “enrichment” is enough for laboratory
537 rodents? A systematic review and meta-analysis re-assessing the impact of well-
538 resourced cages on morbidity and mortality. *Appl Anim Behav Sci* 278:106361.
- 539 Cang J, Kalatsky VA, Löwel S, Stryker MP (2005) Optical imaging of the intrinsic signal as a
540 measure of cortical plasticity in the mouse. *Vis Neurosci* 22:685–691.
- 541 De Bono JP, Adlam D, Paterson DJ, Channon KM (2006) Novel quantitative phenotypes of
542 exercise training in mouse models. *Am J Physiol-Regul Integr Comp Physiol*
543 290:R926–R934.
- 544 Di Garbo A, Mainardi M, Chillemi S, Maffei L, Caleo M (2011) Environmental enrichment
545 modulates cortico-cortical interactions in the mouse. *PLoS ONE* 6.
- 546 Espinosa JS, Stryker MP (2012) Development and Plasticity of the Primary Visual Cortex.
547 *Neuron* 75:230–249.
- 548 Fabel K, Wolf S, Ehninger D, Babu H, Galicia P, Kempermann G (2009) Additive effects of
549 physical exercise and environmental enrichment on adult hippocampal neurogenesis
550 in mice. *Front Neurosci* 3.
- 551 Gordon JA, Stryker MP (1996) Experience-Dependent Plasticity of Binocular Responses in
552 the Primary Visual Cortex of the Mouse. *J Neurosci* 16:3274–3286.
- 553 Greifzu F, Pielecka-Fortuna J, Kalogeraki E, Krempler K, Favaro PD, Schlüter OM, Löwel S
554 (2014) Environmental enrichment extends ocular dominance plasticity into adulthood

- 555 and protects from stroke-induced impairments of plasticity. *Proc Natl Acad Sci U S A*
556 111:1150–1155.
- 557 He H-Y, Hodos W, Quinlan EM (2006) Visual Deprivation Reactivates Rapid Ocular
558 Dominance Plasticity in Adult Visual Cortex. *J Neurosci* 26:2951–2955.
- 559 Hofer SB, Mrsic-Flogel TD, Bonhoeffer T, Hübener M (2006) Lifelong learning: ocular
560 dominance plasticity in mouse visual cortex. *Curr Opin Neurobiol* 16:451–459.
- 561 Hosang L, Yusifov R, Löwel S (2018) Long-Term Visual Training Increases Visual Acuity and
562 Long-Term Monocular Deprivation Promotes Ocular Dominance Plasticity in Adult
563 Standard Cage-Raised Mice. *eneuro* 5:ENEURO.0289-17.2017.
- 564 Hübener M, Bonhoeffer T (2014) Neuronal Plasticity: Beyond the Critical Period. *Cell*
565 159:727–737.
- 566 Iannello F (2019) Non-intrusive high throughput automated data collection from the home
567 cage. *Heliyon* 5:e01454.
- 568 Kalogeraki E, Greifzu F, Haack F, Löwel S (2014) Voluntary physical exercise promotes
569 ocular dominance plasticity in adult mouse primary visual cortex. *J Neurosci*
570 34:15476–15481.
- 571 Kaneko M, Stryker MP (2014) Sensory experience during locomotion promotes recovery of
572 function in adult visual cortex Nelson SB, ed. *eLife* 3:e02798.
- 573 Karnani MM, Schöne C, Bracey EF, González JA, Viskaitis P, Li H-T, Adamantidis A,
574 Burdakov D (2020) Role of spontaneous and sensory orexin network dynamics in
575 rapid locomotion initiation. *Prog Neurobiol*:101771.
- 576 Kempermann G (2019) Environmental enrichment, new neurons and the neurobiology of
577 individuality. *Nat Rev Neurosci* 20:235–245.
- 578 Kopp C (2001) Locomotor activity rhythm in inbred strains of mice: implications for
579 behavioural studies. *Behav Brain Res* 125:93–96.
- 580 Körholz JC, Zocher S, Grzyb AN, Morisse B, Poetzsch A, Ehret F, Schmied C, Kempermann
581 G (2018) Selective increases in inter-individual variability in response to
582 environmental enrichment in female mice. *eLife* 7:e35690.
- 583 Kosse C, Schöne C, Bracey E, Burdakov D (2017) Orexin-driven GAD65 network of the
584 lateral hypothalamus sets physical activity in mice. *Proc Natl Acad Sci* 114:4525–
585 4530.
- 586 Koteja P, Swallow JG, Carter PA, Garland Jr Theodore (1999) Energy Cost of Wheel
587 Running in House Mice: Implications for Coadaptation of Locomotion and Energy
588 Budgets. *Physiol Biochem Zool Ecol Evol Approaches* 72:238–249.
- 589 Lehmann K, Löwel S (2008) Age-dependent ocular dominance plasticity in adult mice. *PLoS*
590 ONE 3.
- 591 Löwel S, Dehmel S, Makowiecki K, Kalogeraki E (2017) Environmental conditions strongly
592 affect brain plasticity. *Neuroforum* 24:A19–A29.

- 593 Manzanares G, Brito-da-Silva G, Gandra PG (2018) Voluntary wheel running: patterns and
594 physiological effects in mice. *Braz J Med Biol Res* 52:e7830.
- 595 Matthies U, Balog J, Lehmann K (2013) Temporally Coherent Visual Stimuli Boost Ocular
596 Dominance Plasticity. *J Neurosci* 33:11774–11778.
- 597 Mayr KA, Young L, Molina LA, Tran MA, Whelan PJ (2020) An economical solution to record
598 and control wheel-running for group-housed mice. *J Neurosci Methods* 331:108482.
- 599 Nguemeni C, McDonald MW, Jeffers MS, Livingston-Thomas J, Lagace D, Corbett D (2018)
600 Short- and Long-term Exposure to Low and High Dose Running Produce Differential
601 Effects on Hippocampal Neurogenesis. *Neuroscience* 369:202–211.
- 602 Pham TA (2004) A semi-persistent adult ocular dominance plasticity in visual cortex is
603 stabilized by activated CREB. *Learn Mem* 11:738–747.
- 604 Plenz UT, Kanold PO (2021) Differences in running performance of single- and group-
605 housed mice. :2021.12.29.474296.
- 606 Prusky GT, Alam NM, Beekman S, Douglas RM (2004) Rapid Quantification of Adult and
607 Developing Mouse Spatial Vision Using a Virtual Optomotor System. *Investig
608 Ophthalmology Vis Sci* 45:4611.
- 609 Reuser A, Wenzel K, Felix SB, Dörr M, Bahls M, Könemann S (2022) Simultaneous
610 assessment of spontaneous cage activity and voluntary wheel running in group-
611 housed mice. *Sci Rep* 12:4444.
- 612 Rhodes JS, Garland T, Gammie SC (2003) Patterns of Brain Activity Associated With
613 Variation in Voluntary Wheel-Running Behavior. *Behav Neurosci* 117:1243–1256.
- 614 Sale A, Maya Vetencourt JF, Medini P, Cenni MC, Baroncelli L, De Pasquale R, Maffei L
615 (2007) Environmental enrichment in adulthood promotes amblyopia recovery through
616 a reduction of intracortical inhibition. *Nat Neurosci* 10:679–681.
- 617 Sato M, Stryker MP (2008) Distinctive features of adult ocular dominance plasticity. *J
618 Neurosci Off J Soc Neurosci* 28:10278–10286.
- 619 Sawtell NB, Frenkel MY, Philpot BD, Nakazawa K, Tonegawa S, Bear MF (2003) NMDA
620 Receptor-Dependent Ocular Dominance Plasticity in Adult Visual Cortex. *Neuron*
621 38:977–985.
- 622 Sherwin CM (1998) Voluntary wheel running: a review and novel interpretation. *Anim Behav*
623 56:11–27.
- 624 Stodieck SK, Greifzu F, Goetze B, Schmidt K-F, Löwel S (2014) Brief dark exposure
625 restored ocular dominance plasticity in aging mice and after a cortical stroke. *Exp
626 Gerontol* 60:1–11.
- 627 Stryker MP, Löwel S (2018) Amblyopia: New molecular/pharmacological and environmental
628 approaches. *Vis Neurosci* 35:E018.
- 629 Wahlsten D, Bachmanov A, Finn DA, Crabbe JC (2006) Stability of inbred mouse strain
630 differences in behavior and brain size between laboratories and across decades.
631 *Proc Natl Acad Sci* 103:16364–16369.

632 Williamson CM, Lee W, DeCasien AR, Lanham A, Romeo RD, Curley JP (2019) Social
633 hierarchy position in female mice is associated with plasma corticosterone levels and
634 hypothalamic gene expression. *Sci Rep* 9:7324.

635

636 Tables

637

638 Table 1: Hardware essentials for building a gated running wheel setup.

Item	Catalog No.	Company
Raspberry pi 4B+ 4GB, 32 GB SD	RP-4B-4GB	Raspberry Pi Foundation, Cambridge, England
Raspberry Pi Noir Camera 2.0 8MP	RB-CAMERAV2IR	Raspberry Pi Foundation, Cambridge, England
Raspberry Pi® RB-LCD-7 Display-Modul 17.8 cm (7 Zoll) 800 x 480 Pixel	RB-LCD-7	Raspberry Pi Foundation, Cambridge, England
RFID reader	ID-20LA	SparkFun Electronics, Colorado, USA
RFID implants	SEN-09416	Sparkfun Electronics, Colorado, USA
roller switch for seesaw	190.072.013	Marquardt, Germany
phototransistor for beam break sensors	BPV11F	Vishay, Germany
reed contact for Hall sensor	MS-213-3	PIC Proximity Instrument Controls GmbH, Germany

639 Figure legends

640

641 **Figure 1. Gated running wheel setup allows to track individual mouse running**
642 **wheel activity.**

643 **A.** Standard-sized rat cage (left, 43 cm x 27 cm) with an additional compartment (right)
644 containing beam break sensors (1,3), a seesaw (2), RFID sensor (4), hall sensor (5),
645 magnet (6), and a running wheel (7). All the sensors are connected to a raspberry pi
646 4B+ (8). (9) Illustrates the size of the implanted RFID.

647 **B.** Comparison of average daily running activity of gRW housed mice (orange) with
648 published data from Kalogeraki et al. 2014 (black).

649 **C.** Example of quantified gRW-activity of two co-housed mice illustrating allocation of
650 running bouts to individual mice (orange/black line) for 2 consecutive days and nights
651 (grey background) (top) and 60 minutes during night time (bottom), with detected
652 running bouts highlighted in grey.

653 **D.** Daily (left) and cumulative (right) running trajectories of individual mice housed in
654 gRW enrichment for 7 days, document a large range of individual running behaviour.

655 While some mice achieve high distances from the first day, for most mice daily running
656 distances only achieved high distances towards the end of the 7 days. Colours of
657 traces and dots are matched for individual mice across figures E-G
658 **E.** Overall there was a significant increase in daily running between day 1 and day 7,
659 but not day 1 and 4.
660 **F.** Running distances of all animals across 7 days binned per hour with top: heat map
661 of individual mice and bottom: average distances across all animals, with overlaid
662 proportion of mice running on each day (defined as at least 1 bin above 0 distance
663 travelled). Note that animals with sufficient running activity predominantly run during
664 night time (higher average values and darker patches in heatmap), with few
665 exceptions of running also during the light period.
666 **G.** Running wheel parameters in individual mice. Note the huge interindividual
667 variability across parameters. Mice that ran longer distances also spent more time
668 running at higher speeds with larger bout numbers.
669 **H.** Correlation matrix illustrating interdependencies of 5 running wheel parameters
670 displayed in G.
671

672 **Figure 2. gRW enrichment boosts ocular dominance plasticity in group-housed
673 mice.**

674 **A.** Intrinsic signal optical imaging examples of grey-scale coded activity maps after
675 visual stimulation of the contralateral and ipsilateral eye in binocular V1 of C57Bl/6J
676 gRW housed mice after 7 days of monocular deprivation (MD) and without MD (no
677 MD). The magnitude of V1-activation is expressed as the fractional change in
678 reflectance $\times 10^{-4}$ and indicated in the top right. Warm colors in the color-coded OD-
679 maps indicate contralateral eye dominance, colder colors indicate an OD-shift towards
680 to ipsilateral eye. Histograms in A,E represent distribution of pixel wise OD-scores.
681 Scale bar: 1mm.
682 **B.** Quantification of OD-index. Symbols represent values of individual mice, means
683 are marked by horizontal lines.
684 **C.** V1-activation elicited by stimulation of the contralateral (C) or ipsilateral (I) eye
685 (filled circle indicates MD eye). Note that MD did not reduce V1-activation through the
686 deprived eye in C.
687 **D.** Spatial frequency threshold of the optomotor reflex for noMD and MD mice, plotted
688 vs. days (x-axis). Note that thresholds increase after MD, indicating successfully
689 induced MD (* $p < 0.05$, ** $p < 0.01$, *** $p < 0.001$ and **** $p < 0.0001$ in Mann-Whitney
690 or 2-way ANOVA with Sidak's post hoc test).
691

692 **Figure 3. Individual running wheel (RW) activity correlates with ocular
693 dominance (OD) plasticity, quantified via the OD-index after monocular
694 deprivation (MD) in P160 mice.**

695 **A.** Example intrinsic signal optical imaging recordings from noMD and MD P160
696 animals, with low (gRW activity <0) and high (gRW activity >0) RW performance (gRW
697 activity was defined as the first principal component (PC1) of RW parameters
698 displayed in C, and shown in B). Data displayed as in figure 2A. Note that OD-
699 plasticity after MD is only boosted in P160 mice, when mice run sufficiently in the gRW
700 setup.
701 **B.** The OD-index of individual P160 mice is correlated with their individual gRW
702 activity after MD (orange), but not in no MD control mice (grey). Lines represent linear
703 regression fitted to MD mice and no MD mice, respectively. Pearson r-values and p-
704 values for MD mice are in the figure.

705 **C.** The OD-index of individual mice after MD is correlated with all quantified running
706 wheel parameters. Data is displayed as in B. Pearson correlation between OD-index
707 and individual wheel running activity was significant for all tested running wheel
708 parameters in P160 mice after MD, but not no MD control mice.

709

710 **Video 1.** Video footage of a mouse entering the gated running wheel compartment via
711 flipping a seesaw.

712 **Video 2.** Video footage of a mouse leaving the gated running wheel compartment via
713 flipping a seesaw. Note that its cage mate is blocked from entering the compartment.

714 **Model 1.** 3D model of gated running wheel components

715 **Figure S1.** Electronic circuit of gated running wheel setup

716 **Figure S2.** Illustration of PCA analysis of wheel running parameters averaged across 7
717 days (A-C) and from individual days (D-F). A,D: Data transformed into coordinate
718 system of principal component (PC) 1 and PC 2 and graphical representation of
719 loadings. B,E: Loadings of all 5 PC C,F: Variability explained by each PC.

720 **Figure S3.** Comparison of wheel running parameters between no MD and MD mice.
721 No significant difference was observed.

Figure 1 Gated running wheel setup allows for detailed readout of wheel running behavior in group housed mice

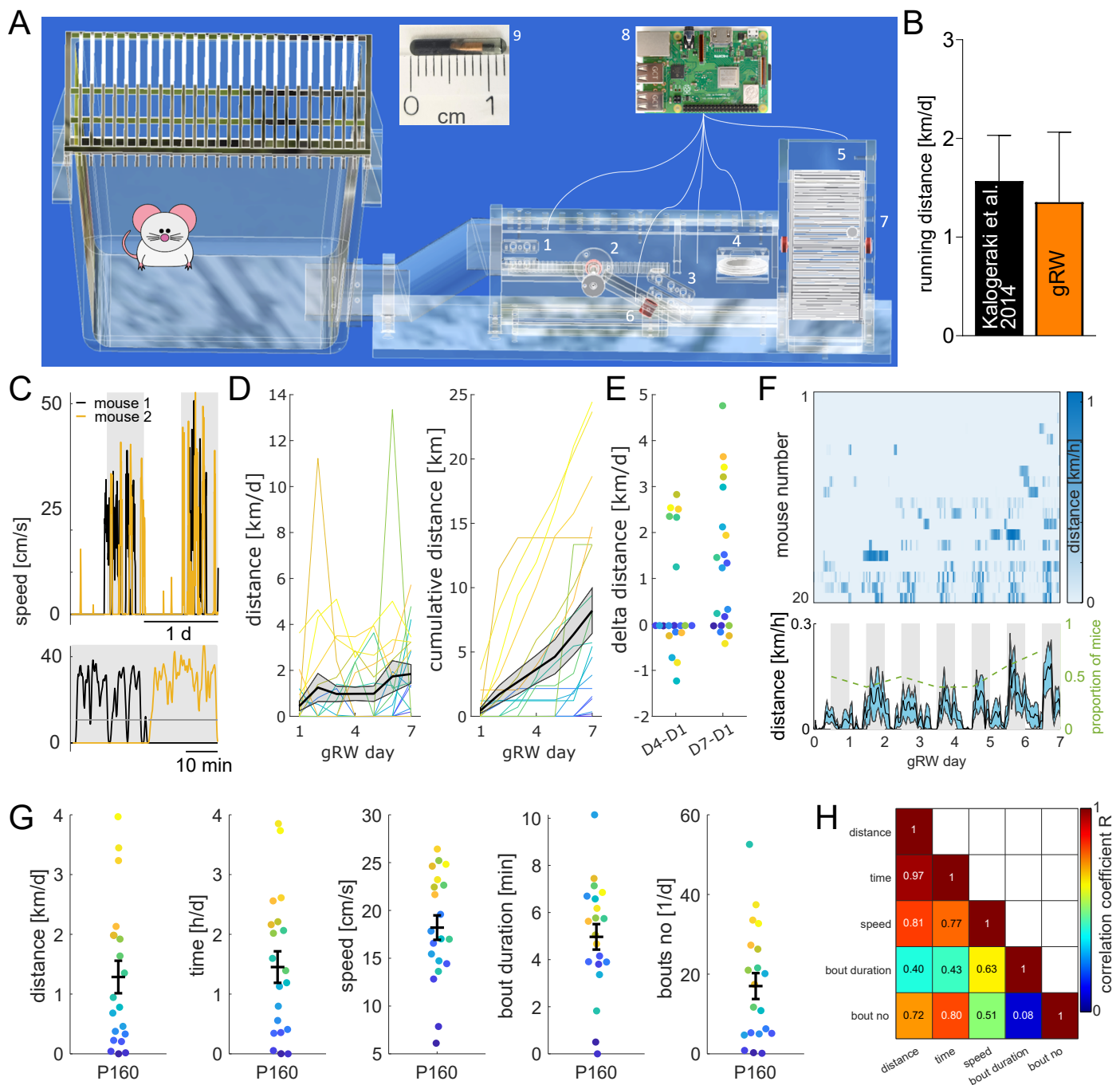


Figure 2 Gated running wheel housing promotes ODP in group housed mice

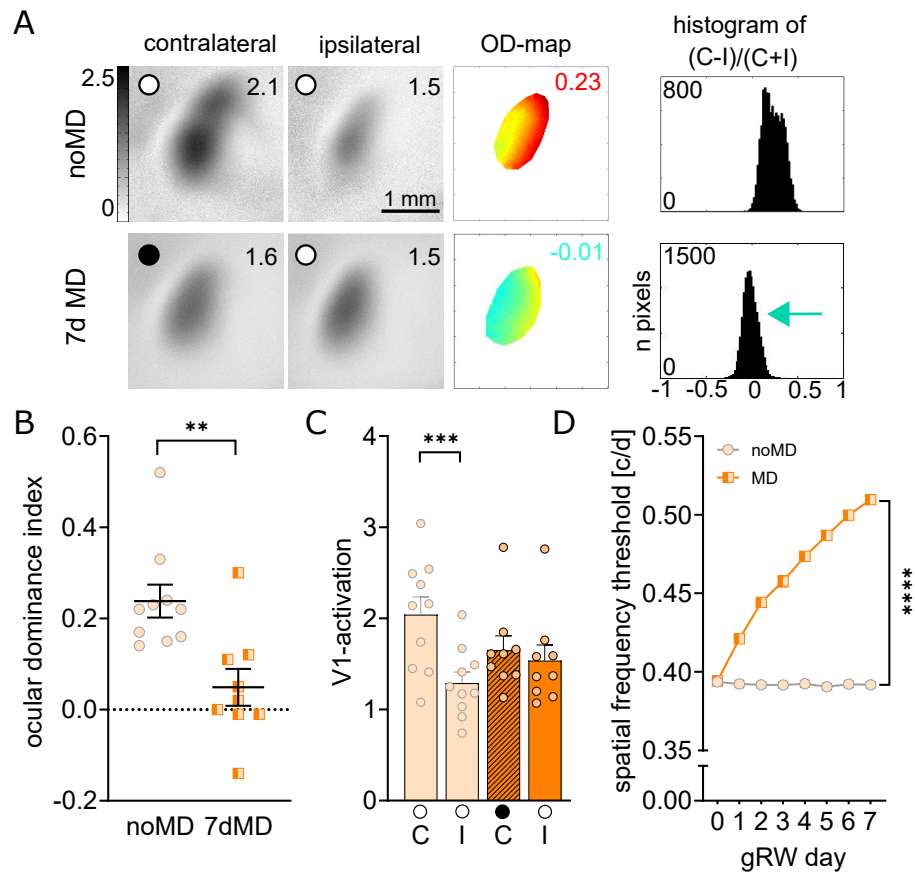


Figure 3 Running wheel activity correlates with ODI

